Interference effects in high-order harmonic generation by homonuclear diatomic molecules

S. Odžak[1] and D. B. Milošević[1,2]
[1]*Faculty of Science, University of Sarajevo, Zmaja od Bosne 35, 71000 Sarajevo, Bosnia and Herzegovina*
[2]*Max-Born-Institut, Max-Born-Strasse 2a, 12489 Berlin, Germany*

(Received 18 October 2008; revised manuscript received 11 December 2008; published 11 February 2009)

A theory of high-order harmonic generation by diatomic molecules is introduced. Various versions (with or without the dressing of the initial and/or final molecular state) of the molecular strong-field approximation are investigated. Using examples of homonuclear diatomic molecules such as H_2, N_2, and O_2, it is shown that clear two-center interference minima in the harmonic spectra as a function of the molecular orientation appear only if the final molecular state is undressed. For H_2 the positions of these minima are in agreement with the *ab initio* numerical results. Physically, the returned electron wave packet recombines into a molecular orbital, which is a linear combination of the atomic orbitals having different parities. The interference minima in the harmonic spectrum are caused by the destructive interference of the corresponding partial recombination amplitudes. In accordance with this, we have derived an interference minima condition which is valid for arbitrary homonuclear diatomic molecules.

DOI: 10.1103/PhysRevA.79.023414 PACS number(s): 33.20.Xx, 42.65.Ky, 42.50.Hz

I. INTRODUCTION

High-order harmonic generation (HHG) is a process in which high-order harmonics of the fundamental laser frequency are coherently radiated when an intense laser pulse is focused into an atomic or molecular gas. This process, discovered in 1987, is usually described by the semiclassical three-step model [1–3]: (i) ionization by the strong laser field, (ii) acceleration of the ionized electron in the laser field, and (iii) recombination of the ionized electron with the parent ion accompanied by the emission of a high-energy photon. More recently, HHG has attracted a lot of attention as a source of coherent radiation in the extreme-ultraviolet and soft-x-ray regions of the spectrum, which can have important applications in attoscience (see, for example, recent reviews [4–7]).

The purpose of the first investigations of HHG by molecular gases in the 1990s was to optimize HHG emission. The main breakthrough in molecular HHG was the discovery of a double-slit-type interference effect in HHG spectra [8]. Theoretically, this was first observed for the simplest diatomic molecules H_2^+ and H_2 [8–11], while experimentally this was first achieved for aligned CO_2 molecules [12,13]. The next major step forward was the so-called tomographic reconstruction of molecular orbitals by Itatani *et al.* [14], where, from the measured spectra at various orientations of the molecular axis, the highest occupied molecular orbital (HOMO) of N_2 was reconstructed. More details and references about molecular imaging can be found in the recent review article by Lein [15]. Its importance for attosecond science and technology was emphasized, for example, in [16,17]. See also the recent Ref. [18] where, using two-dimensional model calculations, the influence of orbital symmetry on HHG and quantum tomography was considered.

The double-slit-type or two-point emitter interference in HHG manifests as minima and maxima in the harmonic yield for particular values of the angle θ_L between the internuclear axis and the laser polarization axis which are accompanied by a jump of the harmonic phase by π. In fact, these two-center interference minima and maxima, respectively, are expected for

$$R\cos\theta_L = (2n+1)\frac{\lambda_k}{2}, \quad R\cos\theta_L = n\lambda_k, \quad n = 0,1,2,\ldots, \tag{1}$$

where R is the internuclear distance and $\lambda_k = 2\pi/k$ is the de Broglie wavelength of the electron having kinetic energy $k^2/(2m)$ equal to the emitted high-harmonic photon energy. This simple model was supported by numerical results for H_2^+ and H_2 [8,9,11,19,20] (see also [21] for a more detailed analysis and [22] for the modification of the interference condition due to the Coulomb effects). However, for more complex diatomic molecules, like N_2 or O_2, this simple physical picture breaks down [23]. The reason is that the HOMO of such molecules can have substantial contributions from atomic orbitals that have different symmetry properties (such as s and p orbitals for N_2). A particularly interesting example is the CO_2 molecule since it has longer internuclear distance, so that the conditions for experimental observation of the interference effect are favorable (we will not consider this triatomic molecule in the present paper; for a review see [15]). More recent measurements of HHG from aligned N_2, O_2, and CO_2 molecules [24] are in contradiction with some of the predictions of the present theoretical models, which motivates further theoretical investigations.

Since *ab initio* HHG calculations for complex molecules thus far have not been possible in any detail, it is clear that sophisticated models and theories have to be developed. The most popular such theories are based on the strong-field approximation (SFA), according to which the electron, between the ionization and recombination, is described by the Volkov states so that its interaction with the laser field is treated exactly, while the influence of the atomic or molecular binding potential is neglected (for example, the Lewenstein model of atomic HHG [3] is such a theory). Generalization of the SFA from atoms to molecules is not so straightforward as one might expect. The main problems are the choice of

gauge and the laser dressing of the bound states. The lack of gauge invariance is much more serious for molecules than for atoms. The problem is common both for HHG and above-threshold ionization [25,26], especially for molecules with large internuclear distances [27]. The length-gauge version of molecular SFA (MSFA) theory of HHG was considered in [28] and references therein, while the velocity-gauge version was studied in [29]. The length-gauge version of MSFA with dressing of both the initial and final bound states was suggested in [30]. The undressed and dressed versions of the SFA were contrasted in the context of HHG during molecular dissociation in [31]. The choice of gauge and the role of dressing in MSFA were also considered in [32,33] and references therein. However, a general consensus has not been reached and it is not clear yet which version of gauge and dressing should be used. In the present paper we will analyze various possibilities.

Some attempts to improve the SFA theories of molecular HHG should be mentioned. The replacement of the plane wave, which appears in the Volkov wave, by the spherical wave in the recombination matrix element was suggested in [34]. Various forms of the recombination and ionization matrix elements can be considered: with dipole operator (this corresponds to length gauge), dipole momentum operator (velocity gauge), and dipole acceleration operator (see [15]). A more general approach which treats a molecule as a multielectron system was developed [35,36] and it was shown that the HOMO should be replaced by the so-called Dyson orbital and that the exchange terms in the dipole matrix element should be included. The Dyson orbital agrees with the Hartree-Fock HOMO up to the second-order many-body perturbation theory [15]. In our paper we will not consider such generalizations of the SFA theory.

It was shown in [37], by direct comparison with the *ab initio* results obtained solving the time-dependent Schrödinger equation, that in the atomic case the length-gauge version of the SFA should be used. The length-gauge version of the molecular SFA is beset by the problem for large internuclear distances which is cured by dressing the initial bound state [27]. Our conclusion is that for the ionization step of the molecular HHG, at least for large internuclear distances, the dressed length gauge should be used. It is known that the recombination matrix element is responsible for the two-center interference, observed in the experiment [15]. We will show that the interference picture depends drastically on the dressing of the final bound state and that only the undressed length-gauge version of the recombination matrix element leads to the appearance of the interference minima at the same positions as in the *ab initio* numerical results for H_2 [8,9] and for the laser intensities used in the experiments with more complex diatomic molecules like N_2 and O_2. We will present an analytical expression for the interference minima condition and this will be the main result of our paper. In Sec. II we present our MSFA theory of HHG, while in Sec. III we will show our numerical results. Our conclusions are given in Sec. IV. The details that are necessary for understanding of our interference condition are relegated to the Appendixes.

II. THEORY OF MOLECULAR HHG

We will describe a diatomic molecule in a laser field using the approach developed in Ref. [25]. The dynamics of our system, which consists of two atomic (ionic) centers A and B and an electron, after the separation of the center-of-mass coordinate $\mathbf{R}_{\mathrm{c.m.}}$, reduces to the relative electron coordinate $\mathbf{r}$ and the relative nuclear coordinate $\mathbf{R}$. The corresponding Hamiltonian is

$$H(t) = \frac{\mathbf{P}^2}{2\mu} + \frac{\mathbf{p}^2}{2m} + V(\mathbf{r},\mathbf{R}) + V_{\mathrm{F}}(\mathbf{r},\mathbf{R},t), \tag{2}$$

where $\mathbf{p}$ and $\mathbf{P}$ are the conjugate momenta that correspond to the Jacobi coordinates $\mathbf{r}$ and $\mathbf{R}$, respectively, $V(\mathbf{r},\mathbf{R})$ is the potential energy of our system in the absence of the laser field, and

$$V_{\mathrm{F}}(\mathbf{r},\mathbf{R},t) = -(e_r\mathbf{r} + e_R\mathbf{R})\cdot\mathbf{E}(t), \tag{3}$$

is the interaction with the laser field in the dipole approximation and the length gauge. The reduces masses μ and m and the relative charges e_r and e_R are defined in [25].

According to the results of Refs. [38,39], the S-matrix element for emission of a harmonic photon having the frequency $\omega_{\mathbf{K}}$, wave vector $\mathbf{K}$, and the polarization $\hat{\mathbf{e}}_{\mathbf{K}}$, is

$$S_{\mathrm{fi}} \propto \int dt\, e^{i(\omega_{\mathbf{K}}t - \mathbf{K}\cdot\mathbf{R}_{\mathrm{c.m.}})}\hat{\mathbf{e}}^*_{\mathbf{K}}\cdot\mathbf{d}_{\mathrm{fi}}(t), \tag{4}$$

where $\mathbf{d}_{\mathrm{fi}}(t)$ is the time-dependent dipole matrix element between the initial and final molecular states in the laser field. For calculation of the harmonic emission rate one has to take into account all possibilities of the initial and final molecular orbitals j' and j, which, in principle, may be different [40], i.e., $S_{\mathrm{fi}} \to \Sigma_{j,j'} S_{jj'}$. However, in most cases we expect that the contribution of the highest occupied molecular orbital is dominant, i.e., $j = j' = \mathrm{HOMO}$. More recently, it has been proposed that the contribution of HOMO-1, HOMO-2, etc., should be taken into account [41] (in our notation this means $S_{\mathrm{fi}} \to \Sigma_j S_{jj}$).

A. Time-dependent dipole

The main contribution to the time-dependent dipole $\mathbf{d}_{\mathrm{fi}}(t)$ in Eq. (4) comes from the matrix element

$$\mathbf{d}^{qq'}_{\mathrm{fi}}(t) = \langle \Phi^q_{\mathrm{f}}(t)|(-e_r\mathbf{r} - e_R\mathbf{R}) \int dt' G^{(+)}(t,t') V_{\mathrm{F}}(\mathbf{r},\mathbf{R},t') \times |\Phi^{q'}_{\mathrm{i}}(t')\rangle, \tag{5}$$

where the retarded Green's operator $G^{(+)}$ corresponds to the Hamiltonian $H(t)$, and $\Phi^q_j(t)$, $j = \mathrm{i},\mathrm{f}$, are the field-free ($q = \mathrm{u}$, undressed) or laser-dressed ($q = \mathrm{d}$, dressed) initial and final molecular bound states. As in [25], we present these states within the Born-Oppenheimer approximation as a product of the electronic state $\phi^q_{\mathrm{e}j}(\mathbf{r},t;\mathbf{R})$ and the nuclear wave function:

$$\Phi^q_j(\mathbf{r},\mathbf{R},t) = \phi^q_{\mathrm{e}j}(\mathbf{r},t;\mathbf{R})\varphi_{AB\nu_j}(\mathbf{R})\exp(-iE_{AB\nu_j}t). \tag{6}$$

For HHG it is not clear yet whether or not the initial and/or final states should be dressed (for different approaches to this

problem see, for example, Refs. [27–33]). One of the aims of the present paper is to explore various possibilities [there are four combinations qq' in Eq. (5)]. The undressed electronic state we present by the linear combination of atomic orbitals (LCAO)

$$\phi^{\mathrm{u}}_{\mathrm{e}j}(\mathbf{r},t;\mathbf{R}) = e^{-iE_{\mathrm{e}j}(\mathbf{R})t}\sum_{J=A,B}\sum_{a} c_{Ja}\psi^{\mathrm{u}}_{a}(\mathbf{r}_J), \tag{7}$$

so that the total energy of the state $\Phi^{\mathrm{u}}_{j}(\mathbf{r},\mathbf{R},t)$ is $E_j(\mathbf{R}) = E_{AB\nu_j} + E_{\mathrm{e}j}(\mathbf{R})$.

In Eq. (7) the sum over a denotes the sum over atomic orbitals, while the sum over J denotes the sum over the molecular centers A and B. Similarly as in [25], the functions $\psi^{\mathrm{u}}_{a}(\mathbf{r}_J) = \psi^{(0)}_{a}(\mathbf{r}_J)$ and the real coefficients c_{Ja} we will represent by the linear combination of the Slater-type orbitals, which are obtained using the Hartree-Fock-Roothan method. For the laser-dressed electronic bound state the atomic orbitals $\psi^{\mathrm{u}}_{a}(\mathbf{r}_J)$ in (7) have to be multiplied by a factor that comes from the potential energy that electron has in the molecular LCAO theory at the position $\mathbf{r}_J$ with respect to the electron position $\mathbf{r}$ in the atomic theory. This potential energy is $e_r\int^t dt' \int^{\mathbf{r}}_{\mathbf{r}_J} d\mathbf{r}\cdot\mathbf{E}(t')$, so that, denoting the vector potential of the laser field by $\mathbf{A}(t) = -\int^t \mathbf{E}(t')dt'$, we have

$$\psi^{\mathrm{d}}_{a}(\mathbf{r}_J) = \psi^{\mathrm{u}}_{a}(\mathbf{r}_J)\exp[-ie_r(\mathbf{r}-\mathbf{r}_J)\cdot\mathbf{A}(t)], \quad \psi^{\mathrm{u}}_{a}(\mathbf{r}_J) = \psi^{(0)}_{a}(\mathbf{r}_J). \tag{8}$$

Let us now return to the time-dependent dipole (5). We will use the strong-field approximation and replace the total Green's operator $G^{(+)}$ by the molecular Volkov Green's operator

$$G^{(+)}_{\mathrm{F}}(t,t') = -i\theta(t-t')\sum_{\nu}\int d^3\mathbf{k}\,|\phi^{\mathrm{F}}_{\mathbf{k}\nu}(t)\rangle\langle\phi^{\mathrm{F}}_{\mathbf{k}\nu}(t')|, \tag{9}$$

where the functions $\phi^{\mathrm{F}}_{\mathbf{k}\nu}(t)$ satisfy the time-dependent Schrödinger equation with the Hamiltonian $H_{\mathrm{F}}(t)$:

$$H_{\mathrm{F}}(t) = h^{\mathrm{F}}_{\mathrm{e}}(t) + H^{\mathrm{F}}_{AB}(t), \quad h^{\mathrm{F}}_{\mathrm{e}}(t) = \frac{\mathbf{p}^2}{2m} - e_r\mathbf{r}\cdot\mathbf{E}(t),$$

$$H^{\mathrm{F}}_{AB}(t) = \frac{\mathbf{P}^2}{2\mu} - e_R\mathbf{R}\cdot\mathbf{E}(t) + V_{AB}(\mathbf{R}). \tag{10}$$

Since the nuclear and electronic coordinates are separated, the function $\Phi^{\mathrm{F}}_{\mathbf{k}\nu}$ can be written as [25]

$$\Phi^{\mathrm{F}}_{\mathbf{k}\nu}(\mathbf{r},\mathbf{R},t) = \phi_{\mathrm{e}\mathbf{k}}(\mathbf{r},t)\varphi_{AB\nu}(\mathbf{R})\exp(-iE_{AB\nu}t), \tag{11}$$

where

$$\phi_{\mathrm{e}\mathbf{k}}(\mathbf{r},t) = (2\pi)^{-3/2}\exp\{i[\mathbf{k}-e_r\mathbf{A}(t)]\cdot\mathbf{r} - iS_{\mathbf{k}}(t)\}, \tag{12}$$

with $S_{\mathbf{k}}(t) = \int^t_{-\infty} d\tau[\mathbf{k}-e_r\mathbf{A}(\tau)]^2/(2m)$, is the electronic Volkov state in the length gauge. The summation in Eq. (9) is over all vibrational degrees of freedom and the integration is over the electron momenta $\mathbf{k}$.

Finally, we fix the internuclear coordinate $\mathbf{R}=\mathbf{R}_0$ in all terms that contain the electronic dependence (this is the so called fixed-nuclei approximation [42]). Then, in our matrix elements, the following overlap integrals between the two vibrational states (we do not consider the rotational dynamics [43]):

$$S_{\mu\nu} = \int d^3\mathbf{R}\,\varphi^{*}_{AB\mu}(\mathbf{R})\varphi_{AB\nu}(\mathbf{R}) \tag{13}$$

will appear. Taking now into account Eqs. (5)–(13), we obtain the following final approximate result for the time-dependent dipole:

$$\mathbf{d}^{qq'}_{\mathrm{fi}}(t) = -ie^{iE_{AB\nu_{\mathrm{f}}}t}\sum_{\nu} S_{\nu_{\mathrm{f}}\nu}S_{\nu\nu_{\mathrm{i}}}e^{-iE_{AB\nu}t}\int_{-\infty}^{t} dt'\,e^{iE_{AB\nu}t' - iE_{AB\nu_{\mathrm{i}}}t'}$$
$$\times\int d^3\mathbf{k}\,e^{i[S_{\mathbf{k}}(t')-S_{\mathbf{k}}(t)]}\langle\phi^{q}_{\mathrm{ef}}(t)|(-e_r\mathbf{r}-e_R\mathbf{R}_0)$$
$$\times|\mathbf{k}-e_r\mathbf{A}(t)\rangle\langle\mathbf{k}-e_r\mathbf{A}(t')|V_{\mathrm{F}}(t')|\phi^{q'}_{\mathrm{ei}}(t')\rangle. \tag{14}$$

B. Harmonic-emission rate for a periodic laser field

For a $(T=2\pi/\omega)$-periodic laser field the rate of emission of a harmonic photon having the frequency $\omega_{\mathbf{K}}=n\omega + E_{\mathrm{i}}(\mathbf{R}_0) - E_{\mathrm{f}}(\mathbf{R}_0)$, wave vector $\mathbf{K}$, and polarization $\hat{\mathbf{e}}_{\mathbf{K}}$, into a solid angle $d\Omega_{\hat{\mathbf{K}}}$, is given by [in atomic units (a.u.)] [38,39]

$$w^{qq'}_{n} = \frac{1}{2\pi}\left(\frac{n\omega}{c}\right)^3|T^{qq'}_{n}|^2, \tag{15}$$

where the T-matrix element $T^{qq'}_{n}$ is

$$T^{qq'}_{n} = \sum_{\nu} S_{\nu_{\mathrm{f}}\nu}S_{\nu\nu_{\mathrm{i}}}T^{qq'}_{n\nu}, \tag{16}$$

with

$$T^{qq'}_{n\nu} = \int_0^T \frac{dt}{T}e^{in\omega t}\hat{\mathbf{e}}^{*}_{\mathbf{K}}\cdot\mathbf{d}^{qq'}_{\nu}(t) \tag{17}$$

and

$$\mathbf{d}^{qq'}_{\nu}(t) = -i\int_{-\infty}^{t} dt'\,e^{i[E_{\mathrm{i}}(\mathbf{R}_0)-E_{AB\nu}](t-t')}\int d^3\mathbf{k}\,e^{i[S_{\mathbf{k}}(t')-S_{\mathbf{k}}(t)]}$$
$$\times\sum_{Ja} c_{Ja}\langle\psi^{q}_{a}(\mathbf{r}_J)|(-e_r\mathbf{r}-e_R\mathbf{R}_0)|\mathbf{k}-e_r\mathbf{A}(t)\rangle$$
$$\times\sum_{J'a'} c_{J'a'}\langle\mathbf{k}-e_r\mathbf{A}(t')|V_{\mathrm{F}}(t')|\psi^{q'}_{a'}(\mathbf{r}_{J'})\rangle. \tag{18}$$

C. HHG of neutral homonuclear diatomic molecules

For neutral homonuclear diatomic molecules such as H_2, N_2, or O_2, we have $\mathbf{r}_J = \mathbf{r} + s\mathbf{R}_0/2 \equiv \mathbf{r}_s$, with $s=+1$ for $J=A$ and $s=-1$ for $J=B$. If the ionization is from the center $J'=A$ $(J'=B)$ we have $e_{R_A}=-\frac{1}{2}$ $(e_{R_B}=+\frac{1}{2})$ so that $V_{\mathrm{F}}(t') = (\mathbf{r} + s'\mathbf{R}_0/2)\cdot\mathbf{E}(t')$ with $s'=+1$ for $J'=A$ and $s'=-1$ for $J'=B$. Analogously, the recombination at the center J is governed by the interaction operator $-e_r\mathbf{r} - e_{R_J}\mathbf{R}_0 = \mathbf{r}_J = \mathbf{r} + s\mathbf{R}_0/2$.

Using the above-mentioned expressions for ψ^{q}_{a}, Eq. (8), and introducing the notation

TABLE I. Equilibrium internuclear distances R_0, ionization energies I_P, initial HOMOs, magnetic quantum number m_a, and atomic orbitals of the used homonuclear diatomic molecules (see Appendix A).

Molecule	R_0 (a.u.)	I_P (eV)	HOMO	m_a	Atomic orbitals
H_2	1.4	16.18	$1\sigma_g$	0	$1s$, $1s'$, $2s$, $2s'$, $3s$, $2p$, $2p'$, $2p''$, $3p$, $3d$, $3d'$, $4f$
N_2	2.068	15.58	$3\sigma_g$	0	$1s$, $1s'$, $2s$, $2s'$, $3s$, $2p$, $2p'$, $2p''$, $3d$, $3d'$, $3d''$, $4f$
O_2	2.282	12.03	$1\pi_g$	1	$2p$, $2p'$, $2p''$, $3d$, $4f$

$$\eta_s^q(\mathbf{k},t) = \begin{cases} e^{-is[\mathbf{k}+\mathbf{A}(t)]\cdot\mathbf{R}_0/2}, & q=\mathrm{u}, \\ e^{-is\mathbf{k}\cdot\mathbf{R}_0/2}, & q=\mathrm{d}, \end{cases} \tag{19}$$

and

$$\mathbf{m}_a(\mathbf{k},t) = \langle \psi_a^{(0)} | \mathbf{r} | \mathbf{k}+\mathbf{A}(t) \rangle, \tag{20}$$

for $T_{n\nu}^{qq'}$, Eq. (17), we obtain

$$T_{n\nu}^{qq'} = -i\int_0^T \frac{dt}{T}\int_{-\infty}^{t} dt' \int d^3\mathbf{k}\, e^{i[S_\nu(\mathbf{k};t,t')+n\omega t]} \times \sum_{sa} c_{sa}\eta_s^q(\mathbf{k},t)\hat{\mathbf{e}}_\mathbf{K}^*\cdot\mathbf{m}_a(\mathbf{k},t) \times \sum_{s'a'} c_{s'a'}\eta_{s'}^{q'*}(\mathbf{k},t')\mathbf{m}_{a'}^*(\mathbf{k},t')\cdot\mathbf{E}(t'), \tag{21}$$

where the action $S_\nu(\mathbf{k};t,t')$ is given by

$$S_\nu(\mathbf{k};t,t') = S_\mathbf{k}(t') - S_\mathbf{k}(t) + [E_i(\mathbf{R}_0) - E_{AB\nu}](t-t'). \tag{22}$$

For numerical calculations we introduce the new variable $\tau = t-t'$ and solve the integral over $\mathbf{k}$ using the saddle-point method [38,39], which gives $\int d^3\mathbf{k} \to [2\pi/(i\tau)]^{3/2}$ and $\mathbf{k} \to \mathbf{k}_{st} = -\int_{t-\tau}^{t}\mathbf{A}(t'')dt''/\tau$ [44]. We neglect the ground-state depletion effect [45].

We will now suppose that the electric field vector changes sign upon a translation in time by $T/2$, i.e.,

$$\mathbf{E}(t+T/2) = -\mathbf{E}(t). \tag{23}$$

This is valid, for example, for a monochromatic linearly polarized laser field having the frequency ω, amplitude E_0, and the unit polarization vector $\hat{\mathbf{e}}_L$: $\mathbf{E}(t)=E_0\hat{\mathbf{e}}_L \sin\omega t$. The vector potential $\mathbf{A}(t)=-\int_{-\infty}^{t}\mathbf{E}(t'')dt''$ obeys the same symmetry: $\mathbf{A}(t+T/2)=-\mathbf{A}(t)$ [for the mentioned example, which we will use in our numerical calculations, we have $\mathbf{A}(t)=A_0\hat{\mathbf{e}}_L\cos\omega t$, $A_0=E_0/\omega$]. For HHG from atoms it is well known that the above symmetry is responsible for the emission of only odd harmonics, since the atomic time-dependent dipole satisfies the relation $\mathbf{d}(t+T/2)=-\mathbf{d}(t)$. In Appendix B we have checked that the same is valid in the molecular case. For odd harmonics n, the T-matrix element is given by Eqs. (B1), (B3), and (B4).

III. NUMERICAL RESULTS

We present harmonic spectra for the H_2, N_2, and O_2 molecules. The corresponding equilibrium internuclear distances, ionization energies, and the parameters which determine the initial HOMOs are presented in Table I. For the H_2 and N_2 molecules, 12 atomic orbitals with $m_a=0$ are taken into account. For s and d states we have $s_{a\lambda}=+1$, while for p and f states it is $s_{a\lambda}=-1$. The $1\pi_g$ HOMO of the O_2 molecule is described by the LCAO of five atomic orbitals having $m_a=1$. In this case, for p and f states we have $s_{a\lambda}=-1$, while for d state it is $s_{a\lambda}=+1$.

A. Harmonic spectra of H_2 and the interference minima condition

As in the atomic case, we expect that our results for the harmonic spectra obtained using the SFA and the saddle-point method are valid for the plateau and cutoff harmonics (see Appendix C). We want to check which of the four possible combinations of the dressed (undressed) initial (final) states give the satisfactory harmonic spectra. For this purpose, in Fig. 1 we present the harmonic spectra of H_2 for $\theta_L=0°$ and for the laser intensity 5×10^{14} W/cm^2 and the wavelength 780 nm. For these parameters, in Refs. [8,9] numerical results are obtained by solving the time-dependent Schrödinger equation for a two-dimensional model of H_2. Figure 2(a) from [8] and Fig. 2(d) from [9] are for the same molecular and laser parameters as our Fig. 1. The harmonic yields, defined as $S(n\omega)=n\omega w_n$, where the rates w_n are given by Eq. (15), are presented as functions of the harmonic order n. The cutoff of the spectrum is at $n_c=71$. For the undressed final state (curves du and uu) the harmonic yield decreases with the decrease of the harmonic order from $n_c=71$ toward a clear minimum at $n_{min}=45$ and then increases [46]. Our results for the du and uu cases are very close to the result presented in [8,9]. However, our results for the dressed final states (ud and dd) are different, which suggests that one should use the MSFA with the undressed final state.

Let us now analyze the interference minima in more detail. In Appendix D it was shown that the saddle-point method leads to the following connection between the harmonic order n and the electron velocity $\mathbf{k}_{st}+\mathbf{A}(t)$ at the rescattering time t: $n\omega=I_P+[\mathbf{k}_{st}+\mathbf{A}(t)]^2/2$ (see the last paragraph of Appendix D for details). The returning electron wave packet recombines into the molecular orbital $1\sigma_g$ which is a linear combination of even and odd atomic orbitals. The corresponding partial recombination amplitudes interfere destructively for the emitted harmonic order, which is the solution of the nonlinear equation

$$n\omega = I_P + \frac{2(j\pi - \arctan z)^2}{R_0^2\cos^2\theta_L}, \quad z = i\frac{\sum_{a_+} c_{1a_+}m_{a_+}}{\sum_{a_-} c_{1a_-}m_{a_-}}, \tag{24}$$

where j is an integer, $z(\theta_L,n)$ is real, and $m_{a_\pm}(\theta_L,n)$ is the component along the laser polarization direction of the di-

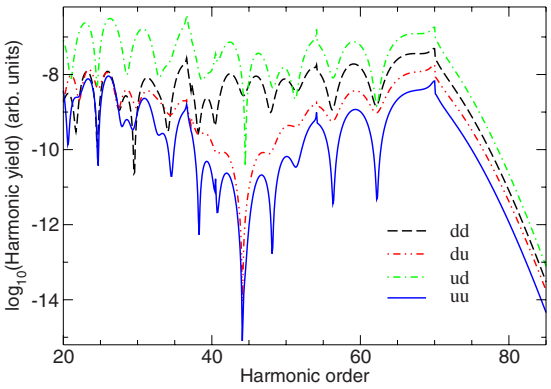

FIG. 1. (Color online) Comparison of the high-order harmonic yields of the H_2 molecule obtained using the four possible combinations of the dressed (undressed) initial (final) molecular bound states. The corresponding results are denoted by the letters dd, du, ud, and uu, where the first letter denotes whether the initial state is dressed (d) or undressed (u), while the second letter characterizes the final state. The laser field intensity is 5×10^{14} W/cm^2 and the wavelength 780 nm. The molecular axis is parallel to the polarization axis of the linearly polarized laser field ($\theta_L=0°$). The yield for the uu case is divided by 10. All results are obtained using the saddle-point method with the first four saddle-point solutions.

pole matrix element (20), $\mathbf{m}_{a_\pm}(\mathbf{k}_{st},t)\equiv m_{a_\pm}(\theta_L,n)\hat{\mathbf{e}}_L$, for the orbitals having $s_{a\lambda}=\pm1$. We have solved Eq. (24) over $n=n_{min}(R_0,\theta_L)$ for the mentioned H_2 example with the undressed final state for fixed $R_0=1.4$ a.u. and for different values of the molecular orientation angle θ_L. In order to compare our results with the results shown in Fig. 3 in [9], in Fig. 2 we present $R_0\cos\theta_L$ as a function of $\lambda=2\pi/\sqrt{2n_{min}\omega}$ [47]. The interference minima curve so obtained (red curve with the circles) follows the line $R_0\cos\theta_L=\lambda/2$. This result is very close to the analogous result obtained in Ref. [9] (open squares in Fig. 3), which confirms our theory.

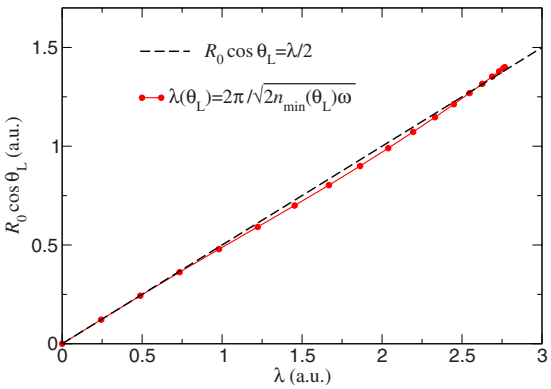

FIG. 2. (Color online) Projected internuclear separation vs effective electron wavelength for HHG by the H_2 molecule. Orientation angle θ_L changes from 0 to 90°, while the other molecular and laser parameters are as in Fig. 1. The results presented by the curve with red circles are obtained by solving Eq. (24) over n_{min} for fixed R_0 and θ_L and presenting $R_0\cos\theta_L$ as a function of $\lambda=2\pi/\sqrt{2n_{min}\omega}$. The dashed line represent the destructive interference condition $R_0\cos\theta_L=(2m+1)\lambda/2$ for $m=0$.

C. Harmonic spectra for N_2

In Fig. 3 we present in false color the harmonic emission rate in the plane (θ_L,n) defined by the angle θ_L between the internuclear axis and the laser polarization axis and by the harmonic order n. The results are presented for all four possible combinations of the dressed (undressed) initial (final) states. Clear two-center interference minima appear only in the case when the final state is undressed. These minima form a curve in the (θ_L,n) plane. It is shown in Appendix D that this curve corresponds to the solutions of the nonlinear equation (24). The curve $n_{min}^{(u)}=n_{min}^{(u)}(\theta_L)$ obtained solving this equation is presented in Figs. 3(b) and 3(d) by a white line. It is evident that it fits very well the false color minima which appear in the numerical results.

In order to show that the relative contribution of even and odd atomic orbitals strongly influences the interference effects in harmonic spectra, in Fig. 4 we present an analog of Fig. 3(b) for the N_2 molecule modeled by either only the s orbitals (left panel) or only the p orbitals (right panel). The interference picture is completely different and is in accordance with Eq. (D2) for $j=0$ [s orbitals, Fig. 4(a)] and Eq. (D3) for $j=1$ [p orbitals, Fig. 4(b)]. These equations are special cases of Eq. (24), as shown in Appendix D.

B. Harmonic spectra for O_2

Since the main contribution to the $1\pi_g$ HOMO of the O_2 molecule comes from the p atomic orbitals, we expect that the interference minima will appear for higher harmonic orders, i.e., higher laser intensities are needed to observe these minima (see the right-hand panel of Fig. 4). Therefore, in Fig. 5 we present harmonic spectra for the laser intensity 6×10^{14} W/cm^2, which is higher than that used in Figs. 3 and 4. We again see that only the combinations with the undressed final state lead to clear interference minima. Furthermore, these interference minima are very well described by the solution of the nonlinear Eq. (24) for $j=-1$. These solutions are presented by white lines in Figs. 5(b) and 5(d).

In Fig. 5 one can also notice the minima for parallel ($\theta_L=0°$) and perpendicular ($\theta_L=\pm90°$) orientations. These minima are connected with the $1\pi_g$ symmetry of the HOMO of the O_2 molecule and are clearly visible for all harmonic orders and for all combinations of the dressed (undressed) initial (final) states.

IV. CONCLUSION

We have presented a theory of high-order harmonic generation of a diatomic molecule which is considered as a system of two atomic (ionic) centers and one electron. The dynamics of this system is described by the relative electron coordinate and the relative nuclear coordinate. The electronic state is presented by the linear combination of atomic orbitals. The theory is formulated in such a way that the strong-field approximation with the laser-field dressed or undressed initial and final states can be treated on the same footing. This enables us to compare different versions of the molecular SFA. We have shown that clear two-center interference minima, in agreement with the *ab initio* numerical results,

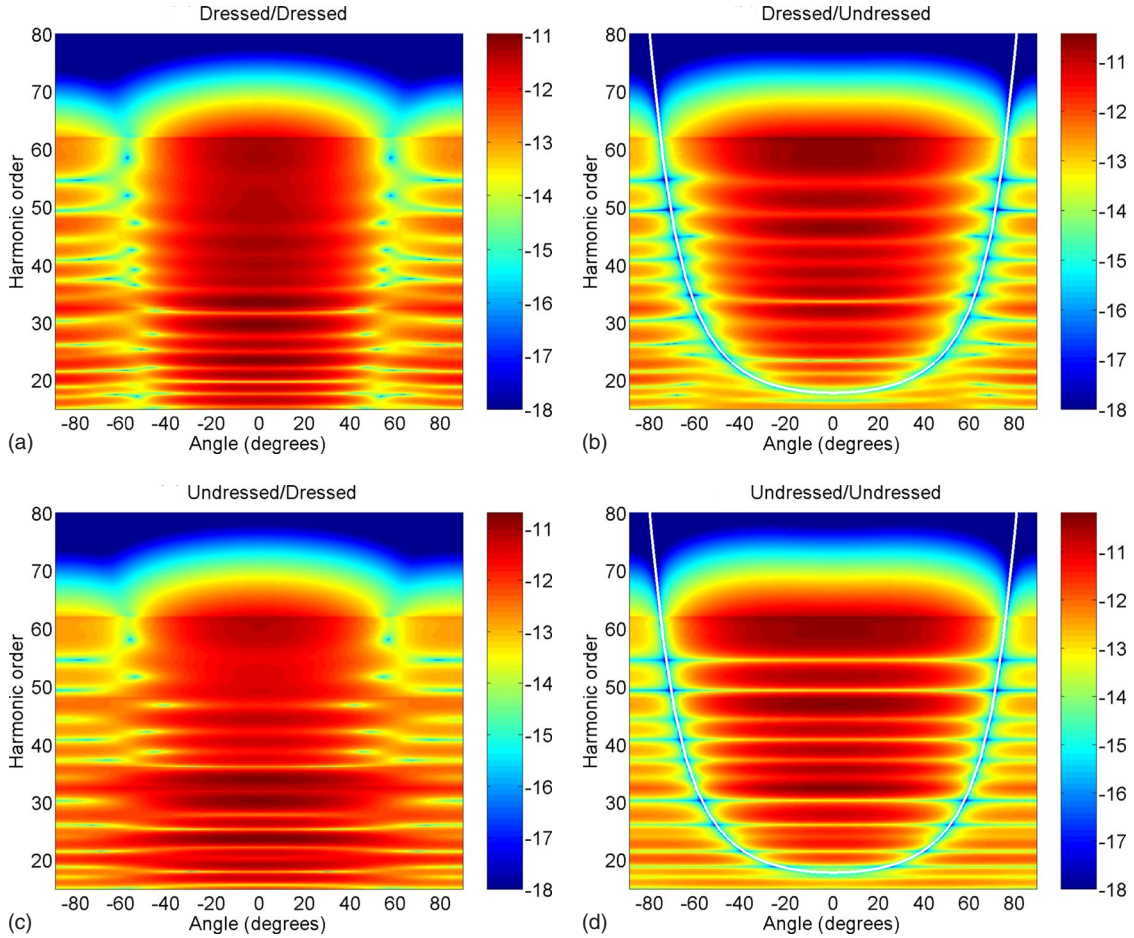

FIG. 3. (Color online) High-order harmonic spectra of the N_2 molecule obtained using a linearly polarized laser field having the intensity 4×10^{14} W/cm^2 and photon energy ω=1.55 eV. (a)–(d) illustrate HHG spectra for the four possible combinations where the initial (final) molecular bound states are dressed (undressed). The angle between the laser field polarization axis and the molecular axis is plotted along the horizontal axis, while the harmonic order is along the vertical axis. The curves $n_{\min}^{(u)}=n_{\min}^{(u)}(\theta_L)$, which express the interference minima condition as the solution of the nonlinear equation defined by Eq. (D10) for j=0, are presented by white lines in (b) and (d).

appear only if the final state is undressed. Therefore, in the final (recombination) step the molecular state should be treated as undressed. As concerns the initial state, we suggest that, at least for large internuclear distances, it should be dressed. This is supported by the following findings. First, for the atomic p ground state, by comparison with the *ab*

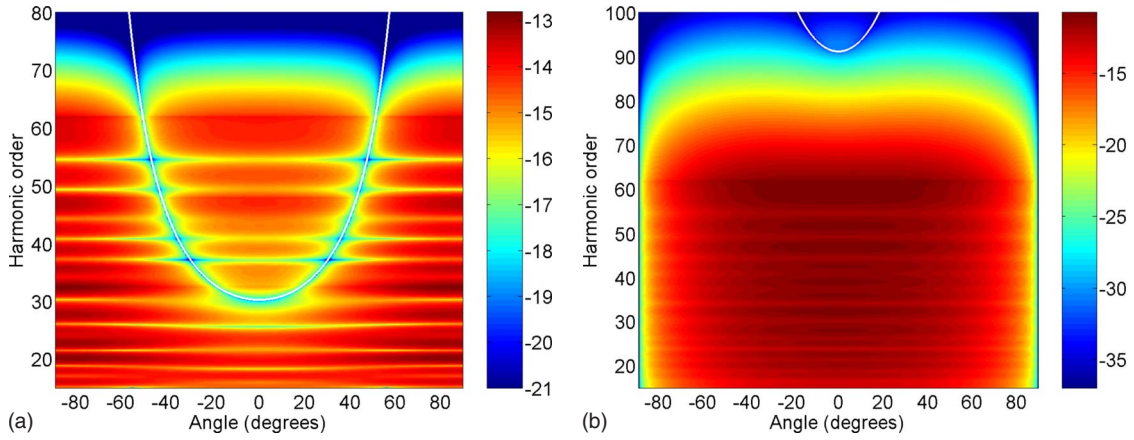

FIG. 4. (Color online) As in Fig. 3 but taking into account only the s orbitals (left panel) and only the p orbitals (right panel). Only the combination with the dressed initial state and the undressed final state is presented. The curve given by Eq. (D2) [Eq. (D3)] is depicted in the left (right) panel by a white line.

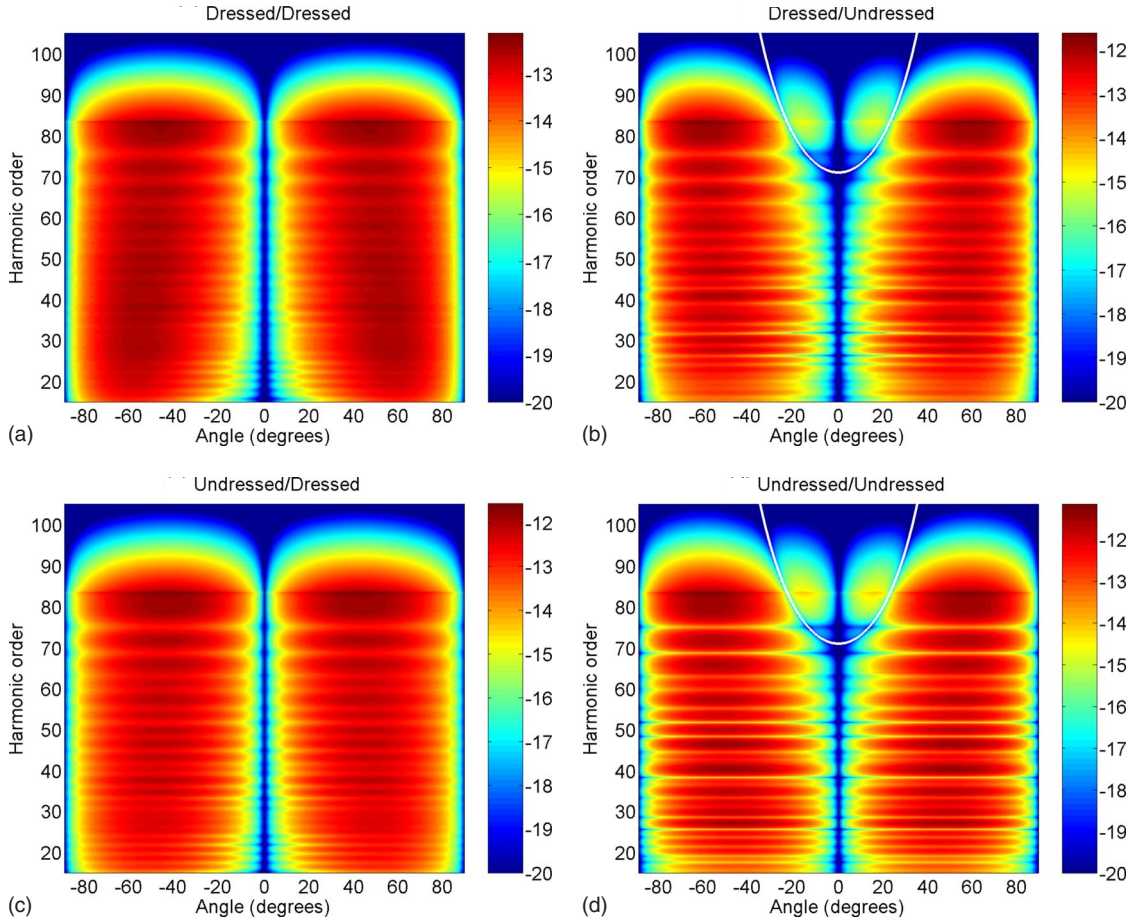

FIG. 5. (Color online) As in Fig. 3 but for the O_2 molecule and the laser intensity 6×10^{14} W/cm^2. The interference minima curves $n_{\min}^{(u)}=n_{\min}^{(u)}(\theta_L)$ in (b) and (d) are the solutions of Eq. (D10) for $j=-1$.

initio results, it was shown that only the SFA in its length-gauge version gives the correct results [37]. Second, in Ref. [27] it was shown that if one uses the length gauge in consideration of the ionization process and if the internuclear distance is large, then the molecular ground state should be dressed.

We mentioned in the Introduction that for more complex diatomic molecules the simple physical picture based on the two-center interference formula (1) breaks down. Since our theory is general it can be applied to arbitrary diatomic molecules. We have derived a general two-center interference formula (24) [see also Eq. (D10)] which is a nonlinear equation for the harmonic order as a function of the internuclear distance and the molecular orientation angle. This formula contains the ratio of the sum of the dipole matrix elements with even and odd atomic orbitals whose linear combination forms the molecular orbital from which the high harmonics are emitted. Our numerical results for the H_2 (Fig. 1), N_2 (Figs. 3 and 4), and O_2 (Fig. 5) molecules are in excellent agreement with this interference minima condition. The physical explanation of the results obtained is the following: in the third step of the three-step model of HHG the returned electron wave packet recombines into the HOMO which is a linear combination of even and odd atomic orbitals. The destructive interference of even (A_+) and odd (A_-) partial recombination amplitudes [see Eqs. (D8) and (D9)] is responsible for the observed minima. The positions of these minima depend on the ratio of the summed dipole matrix element, determined by the real parameter $z=iA_+/A_-$, Eqs. (D9) and (D10).

ACKNOWLEDGMENTS

This work was supported in part by the VolkswagenStiftung and by the Federal Ministry of Education and Science, Bosnia and Herzegovina.

APPENDIX A: DIPOLE MATRIX ELEMENTS FOR THE MOLECULAR ORBITAL WAVE FUNCTIONS

For the ground-state electronic wave functions of the neutral homonuclear diatomic molecules we use the Hartree-Fock-Roothaan wave functions [25]

$$\phi_{ej}(\mathbf{r};\mathbf{R})=\sum_{s=\pm1}\sum_{a}c_{sa}\psi_a(\mathbf{r}+s\mathbf{R}/2), \tag{A1}$$

with $\psi_a(\mathbf{r})$ the Slater-type orbitals

$$\psi_a(\mathbf{r})=\frac{(2\zeta_a)^{n_a+1/2}}{\sqrt{(2n_a)!}}r^{n_a-1}e^{-\zeta_a r}Y_{l_a m_a}(\theta,\varphi)=\varphi_{n_a}(r)Y_{l_a m_a}(\theta,\varphi). \tag{A2}$$

The method of calculation of the functions (A1) is described in [48,49] and the results for the coefficients $\sqrt{2}c_{1a}$ and the

orbital exponents ζ_a are tabulated in [50,51]. The coefficients at the center B are equal, up to a sign, to the coefficients at the center A, i.e., $c_{-1a}=s_{a\lambda}c_{1a}$, where

$$s_{a\lambda}=(-1)^{l_a-m_a}\begin{cases}(-1)^{m_\lambda} & \text{for g symmetry,}\\ (-1)^{m_\lambda+1} & \text{for u symmetry.}\end{cases} \tag{A3}$$

Here m_a is the magnetic quantum number of the atomic orbital a and $m_\lambda=|m_a|$ is the value of the projection of the orbital angular momentum on the internuclear axis. For example, for σ states it is $m_\lambda=0$, and $m_\lambda=1$ for π states.

For calculation of the harmonic emission rate we need the dipole matrix element, Eq. (20),

$$\mathbf{m}_a^*(\mathbf{k},t)=\langle\mathbf{p}|\mathbf{r}|\psi_a\rangle=i\frac{\partial}{\partial\mathbf{p}}\tilde{\psi}_a(\mathbf{p}),\quad \mathbf{p}=\mathbf{k}+\mathbf{A}(t), \tag{A4}$$

where the momentum-space Slater-type orbitals are defined as the Fourier transform

$$\chi_{n_al_am_a}(p,\theta_p,\phi_p)\equiv\tilde{\psi}_a(\mathbf{p})=(2\pi)^{-3/2}\int d\mathbf{r}\,\exp(-i\mathbf{p}\cdot\mathbf{r})\psi_a(\mathbf{r}). \tag{A5}$$

The analytical solution of this integral is

$$\chi_{n_al_am_a}(\mathbf{p})=\frac{2^{n_a-l_a}\Gamma(2+n_a+l_a)}{\sqrt{(2n_a)!}\Gamma\left(\frac{3}{2}+l_a\right)}\zeta_a^{-3/2-l_a}(-ip)^{l_a}\times{}_2F_1\left(\frac{1}{2}(2+l_a+n_a),\frac{1}{2}(3+l_a+n_a);\frac{3}{2}+l_a;-\frac{p^2}{\zeta_a^2}\right)Y_{l_am_a}(\theta_p,\phi_p), \tag{A6}$$

where ${}_2F_1$ are the hypergeometric functions. For the $1\sigma_g$ HOMO of H_2 and the $3\sigma_g$ HOMO of N_2 we will use the following orbitals:

$$\chi_{1s\sigma}(\mathbf{p})\equiv\chi_{100}(\mathbf{p})=\frac{2\sqrt{2}\zeta_{1s}^{5/2}}{\pi}\frac{1}{(p^2+\zeta_{1s}^2)^2},$$

$$\chi_{2s\sigma}(\mathbf{p})\equiv\chi_{200}(\mathbf{p})=-\frac{2\sqrt{2}\zeta_{2s}^{5/2}}{\sqrt{3}\pi}\frac{(p^2-3\zeta_{2s}^2)}{(p^2+\zeta_{2s}^2)^3},$$

$$\chi_{3s\sigma}(\mathbf{p})\equiv\chi_{300}(\mathbf{p})=\frac{16\zeta_{3s}^{9/2}}{\sqrt{5}\pi}\frac{(-p^2+\zeta_{3s}^2)}{(p^2+\zeta_{3s}^2)^4},$$

$$\chi_{2p\sigma}(\mathbf{p})\equiv\chi_{210}(\mathbf{p})=-\frac{8i\sqrt{2}\zeta_{2p}^{7/2}}{\pi}\frac{p\cos\theta_p}{(p^2+\zeta_{2p}^2)^3},$$

$$\chi_{3p\sigma}(\mathbf{p})\equiv\chi_{310}(\mathbf{p})=\frac{16i\zeta_{3p}^{7/2}}{\sqrt{15}\pi}\frac{p\cos\theta_p(p^2-5\zeta_{3p}^2)}{(p^2+\zeta_{3p}^2)^4},$$

$$\chi_{3d\sigma}(\mathbf{p})\equiv\chi_{320}(\mathbf{p})=-\frac{16\zeta_{3d}^{9/2}}{\pi}\frac{p^2(3\cos^2\theta_p-1)}{(p^2+\zeta_{3d}^2)^4},$$

$$\chi_{4f\sigma}(\mathbf{p})\equiv\chi_{430}(\mathbf{p})=\frac{64i\sqrt{2}\zeta_{4f}^{11/2}}{\sqrt{5}\pi}\frac{p^3\cos\theta_p(5\cos^2\theta_p-3)}{(p^2+\zeta_{4f}^2)^5}. \tag{A7}$$

The coordinate space wave functions (A1) and the corresponding momentum space wave functions

$$\tilde{\phi}_{ej}(\mathbf{p};\mathbf{R})=\sum_{s=\pm1}\sum_a c_{sa}\exp\left(i\mathbf{p}\cdot s\frac{\mathbf{R}}{2}\right)\chi_{n_al_am_a}(\mathbf{p}), \tag{A8}$$

obtained using these orbitals, are presented in Fig. 2 in [25] for the N_2 molecule.

The factor $e^{im\phi}$ makes the spherical harmonics $Y_{lm}(\theta,\varphi)$ complex, except for $m=0$. Instead of using the normalized complex spherical harmonics

$$Y_{lm}(\theta,\varphi)=(-1)^m\sqrt{\frac{2l+1}{2}\frac{(l-m)!}{(l+m)!}}P_{lm}(\cos\theta)\frac{e^{im\varphi}}{\sqrt{2\pi}}, \tag{A9}$$

where $P_{lm}(\cos\theta)$ are the unnormalized associated Legendre functions [48,49], we will use the real spherical harmonics defined by (see, for example, Appendix A in [52])

$$S_{l|m|}(\theta,\varphi)=P_{l|m|}(\cos\theta)\frac{1}{\sqrt{\pi}}\cos(|m|\varphi),$$

$$S_{l-|m|}(\theta,\varphi)=P_{l|m|}(\cos\theta)\frac{1}{\sqrt{\pi}}\sin(|m|\varphi),$$

$$S_{l0}(\theta,\varphi)=\frac{1}{\sqrt{2\pi}}P_{l0}(\cos\theta). \tag{A10}$$

For example, in order to describe the wave function of the O_2 molecule, we will need the following real spherical harmonics:

$$S_{11}(\theta,\varphi)=\sqrt{\frac{3}{4\pi}}\sin\theta\cos\varphi,$$

$$S_{21}(\theta,\varphi)=\sqrt{\frac{15}{4\pi}}\sin\theta\cos\theta\cos\varphi,$$

$$S_{31}(\theta,\varphi)=\sqrt{\frac{21}{32\pi}}(5\cos^2\theta-1)\sin\theta\cos\varphi. \tag{A11}$$

The HOMO of the O_2 molecule is $1\pi_g$ and the corresponding coordinate and momentum space wave functions are presented in Fig. 3 in [25]. The coordinate wave functions are given by $\varphi_{n_a}(r)S_{l_am_a}(\theta,\varphi)$, $m_a=1$, $n_al_a=2p$, $3d$, and $4f$, while the momentum wave functions are

$$\chi_{2p\pi}(\mathbf{p})=-\frac{2^{9/2}i\zeta_{2p}^{7/2}}{\sqrt{3\pi}}\frac{p}{(p^2+\zeta_{2p}^2)^3}S_{11}(\theta_p,\phi_p),$$

$$\chi_{3d\pi}(\mathbf{p})=-\frac{64\zeta_{3d}^{9/2}}{\sqrt{5\pi}}\frac{p^2}{(p^2+\zeta_{3d}^2)^4}S_{21}(\theta_p,\phi_p),$$

$$\chi_{4f\pi}(\mathbf{p}) = \frac{2^{17/2} i \zeta_{4f}^{11/2}}{\sqrt{35\pi}} \frac{p^3}{(p^2+\zeta_{4f}^2)^5} S_{31}(\theta_p, \phi_p). \quad \text{(A12)}$$

Let us now return to the dipole matrix element (A4) with (A5). In our approach, the intermediate electron momentum $\mathbf{k}=\mathbf{k}_{\rm st}$ is along the polarization axis so that $\partial/\partial\mathbf{p}=\hat{\mathbf{e}}_{\rm L}\partial/\partial p$. Using the results (A7) and (A12) we easily obtain the dipole matrix element that we need to model HHG from the HOMOs of H_2 and N_2,

$$i\frac{\partial}{\partial p}\chi_{1s\sigma}(\mathbf{p}) = -\frac{8i\sqrt{2}\zeta_{1s}^{5/2}}{\pi}\frac{p}{(p^2+\zeta_{1s}^2)^3},$$

$$i\frac{\partial}{\partial p}\chi_{2s\sigma}(\mathbf{p}) = \frac{8i\sqrt{2}\zeta_{2s}^{5/2}}{\sqrt{3}\pi}\frac{p(p^2-5\zeta_{2s}^2)}{(p^2+\zeta_{2s}^2)^4},$$

$$i\frac{\partial}{\partial p}\chi_{3s\sigma}(\mathbf{p}) = \frac{32i\zeta_{3s}^{9/2}}{\sqrt{5}\pi}\frac{p(3p^2-5\zeta_{3s}^2)}{(p^2+\zeta_{3s}^2)^5},$$

$$i\frac{\partial}{\partial p}\chi_{2p\sigma}(\mathbf{p}) = \frac{8\sqrt{2}\zeta_{2p}^{7/2}}{\pi}\frac{\cos\theta_p(-5p^2+\zeta_{2p}^2)}{(p^2+\zeta_{2p}^2)^4},$$

$$i\frac{\partial}{\partial p}\chi_{3p\sigma}(\mathbf{p}) = \frac{16\zeta_{3p}^{7/2}}{\sqrt{15}\pi}\frac{\cos\theta_p(5p^4-38p^2\zeta_{3p}^2+5\zeta_{3p}^4)}{(p^2+\zeta_{3p}^2)^5},$$

$$i\frac{\partial}{\partial p}\chi_{3d\sigma}(\mathbf{p}) = \frac{32i\zeta_{3d}^{9/2}}{\pi}\frac{(3\cos^2\theta_p-1)p(3p^2-\zeta_{3d}^2)}{(p^2+\zeta_{3d}^2)^5},$$

$$i\frac{\partial}{\partial p}\chi_{4f\sigma}(\mathbf{p}) = \frac{64\sqrt{2}\zeta_{4f}^{11/2}}{\sqrt{5}\pi}\frac{p^2\cos\theta_p(5\cos^2\theta_p-3)(7p^2-3\zeta_{4f}^2)}{(p^2+\zeta_{4f}^2)^6}, \quad \text{(A13)}$$

and O_2,

$$i\frac{\partial}{\partial p}\chi_{2p\pi}(\mathbf{p}) = \frac{8\sqrt{2}\zeta_{2p}^{7/2}}{\pi}\frac{(-5p^2+\zeta_{2p}^2)\sin\theta_p\cos\phi_p}{(p^2+\zeta_{2p}^2)^4},$$

$$i\frac{\partial}{\partial p}\chi_{3d\pi}(\mathbf{p}) = \frac{32i\sqrt{3}\zeta_{3d}^{9/2}}{\pi}\frac{p(3p^2-\zeta_{3d}^2)\sin 2\theta_p\cos\phi_p}{(p^2+\zeta_{3d}^2)^5},$$

$$i\frac{\partial}{\partial p}\chi_{4f\pi}(\mathbf{p}) = \frac{32\sqrt{3}\zeta_{4f}^{11/2}}{\sqrt{5}\pi}\frac{p^2(7p^2-3\zeta_{4f}^2)(3+5\cos 2\theta_p)\sin\theta_p\cos\phi_p}{(p^2+\zeta_{4f}^2)^6}. \quad \text{(A14)}$$

The internuclear axis is along the z axis so that we can choose $\theta_p=\theta_{\rm L}$, $\phi_p=0$, where $\theta_{\rm L}$ is the angle between the internuclear axis and the laser polarizaton axis.

APPENDIX B: PROOF THAT ONLY ODD HARMONICS ARE EMITTED FOR THE FIELD (23)

For the electric field $\mathbf{E}(t)$ such that Eq. (23) is satisfied, it is easy to show that the quantities that appear in the T-matrix element (21) for $\omega t\to\omega t+\pi$ transform as $\mathbf{k}_{\rm st}\to-\mathbf{k}_{\rm st}$, $\eta_s^q(\mathbf{k}_{\rm st},t)\to\eta_s^{q^*}(\mathbf{k}_{\rm st},t)=\eta_{-s}^q(\mathbf{k}_{\rm st},t)$, $e^{in\omega t}\to(-1)^n e^{in\omega t}$, $S_\nu\to S_\nu$, $\mathbf{m}_a(\mathbf{k}_{\rm st},t)\to(-1)^{l_a+1}\mathbf{m}_a(\mathbf{k}_{\rm st},t)$, where l_a is the orbital quantum number of the atomic orbital a. Using this, we obtain that Eq. (21) reduces to

$$T_{n\nu}^{qq'} = -i\left(\frac{2\pi}{i}\right)^{3/2}\int_0^{T/2}\frac{dt}{T}e^{in\omega t}\int_0^\infty\frac{d\tau}{\tau^{3/2}}e^{iS_\nu(\mathbf{k}_{\rm st};t,t-\tau)} \times\sum_{a,a'}\mathbf{m}_a(\mathbf{k}_{\rm st},t)\cdot\hat{\mathbf{e}}_{\mathbf{K}}^*\mathbf{m}_{a'}^*(\mathbf{k}_{\rm st},t-\tau)\cdot\mathbf{E}(t-\tau) \times f_{naa'}^{qq'}(\mathbf{k}_{\rm st};t,t-\tau), \quad \text{(B1)}$$

where

$$f_{naa'}^{qq'}(\mathbf{k}_{\rm st};t,t-\tau) = \sum_{s,s'}c_{sa}c_{s'a'}[\eta_s^q(\mathbf{k}_{\rm st},t)\eta_{-s'}^{q'}(\mathbf{k}_{\rm st},t-\tau) - (-1)^n(-1)^{l_a+l_{a'}}\eta_{-s}^q(\mathbf{k}_{\rm st},t)\eta_{s'}^{q'}(\mathbf{k}_{\rm st},t-\tau)]. \quad \text{(B2)}$$

In order to perform the summation over s and s' we will use the fact that the coefficients c_{sa} of our molecular orbitals satisfy the relation $c_{-1a}=s_{a\lambda}c_{1a}$ [25,26] [see Eq. (A3); $m_\lambda=|m_a|=|m_{a'}|$]. Using this we calculate separately $s=s'$ and $s\neq s'$ contributions to the sums in Eq. (B2). For $s=s'$ we obtain

$$c_{1a}c_{1a'}[1-(-1)^n][\eta_1^q(\mathbf{k}_{\rm st},t)\eta_{-1}^{q'}(\mathbf{k}_{\rm st},t-\tau) + (-1)^{l_a+l_{a'}}\eta_{-1}^q(\mathbf{k}_{\rm st},t)\eta_1^{q'}(\mathbf{k}_{\rm st},t-\tau)],$$

while for the sum of two terms with $s\neq s'$ we find

$$c_{1a}c_{1a'}[1-(-1)^n][s_{a'\lambda}\eta_1^q(\mathbf{k}_{\rm st},t)\eta_1^{q'}(\mathbf{k}_{\rm st},t-\tau) + s_{a\lambda}\eta_{-1}^q(\mathbf{k}_{\rm st},t)\eta_{-1}^{q'}(\mathbf{k}_{\rm st},t-\tau)].$$

Therefore, only odd harmonics n are emitted and the corresponding T-matrix element is given by Eq. (B1) with

$$f_{naa'}^{qq'}(\mathbf{k}_{\rm st};t,t-\tau) = 2c_{1a}c_{1a'}F_{s_{a\lambda}}^q(\mathbf{k}_{\rm st},t)F_{s_{a'\lambda}}^{q'*}(\mathbf{k}_{\rm st},t-\tau), \quad \text{(B3)}$$

where

$$F_{s_{a\lambda}}^q = \eta_1^q + s_{a\lambda}\eta_{-1}^q. \quad \text{(B4)}$$

For $s_{a\lambda}=+1$ the factor F_{+1}^q reduces to $2\cos[\mathbf{K}^q(\mathbf{k}_{\rm st},t)\cdot\mathbf{R}_0/2]$, while for the $s_{a\lambda}=-1$ for F_{-1}^q we obtain $-2i\sin[\mathbf{K}^q(\mathbf{k}_{\rm st},t)\cdot\mathbf{R}_0/2]$, with

$$\mathbf{K}^q(\mathbf{k}_{\rm st},t) = \begin{cases}\mathbf{k}_{\rm st}+\mathbf{A}(t), & q=\mathrm{u},\\ \mathbf{k}_{\rm st}, & q=\mathrm{d}.\end{cases} \quad \text{(B5)}$$

APPENDIX C: SADDLE-POINT METHOD

Application of the saddle-point method to the T-matrix element (21) leads to the condition that the partial derivatives over $\mathbf{k}$, t', and t of the action $S_{n\nu}^{qq'}(\mathbf{k};t,t')+n\omega t$ are equal to

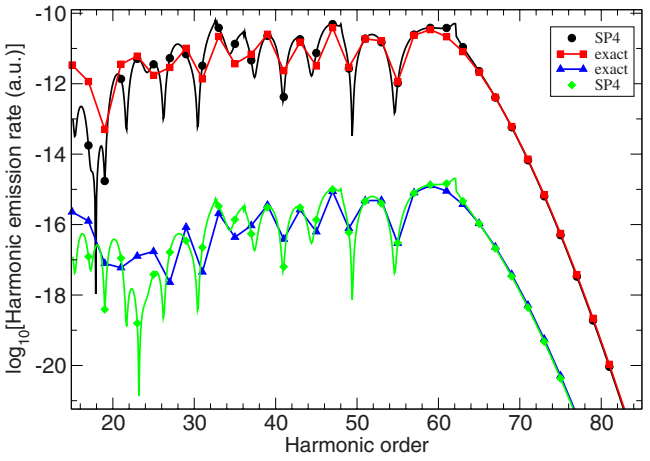

FIG. 6. (Color online) Comparison of the high-order harmonic spectra of the N_2 molecule obtained using the saddle-point method with the first four saddle-point solutions (circles and diamonds denoted by "SP4") and the "exact" spectra obtained using numerical integration (squares and triangles). The laser field is linearly polarized having the intensity 4×10^{14} W/cm^2 and photon energy $\omega=1.55$ eV. For the black curve with circles and red curve with squares the angle between the internuclear axis and the laser polarization axis is $\theta_L=0°$, while for the green curve with diamonds and blue curve with triangles it is $\theta_L=45°$, and these curves are shifted down by four orders of magnitude.

zero, which gives $\mathbf{k}=\mathbf{k}_{st}\equiv-\int_{t'}^{t}\mathbf{A}(t'')dt''/(t-t')$ and the following system of equations for the variables t' and t:

$$\frac{1}{2}[\mathbf{k}_{st}+\mathbf{A}(t')]^2=E_i(\mathbf{R}_0)-E_{AB\nu}=E_{ei}(\mathbf{R}_0)+E_{AB\nu_i}-E_{AB\nu}, \tag{C1}$$

$$\begin{aligned}\frac{1}{2}[\mathbf{k}_{st}+\mathbf{A}(t)]^2&=n\omega+E_i(\mathbf{R}_0)-E_{AB\nu}\\&=n\omega+E_{ei}(\mathbf{R}_0)+E_{AB\nu_i}-E_{AB\nu}\\&=\omega_{\mathbf{K}}+E_{ef}(\mathbf{R}_0)+E_{AB\nu_f}-E_{AB\nu}.\end{aligned} \tag{C2}$$

For simplicity, in our calculations we suppose that $\nu=\nu_i=\nu_f$ and $E_{ei}(\mathbf{R}_0)=E_{ef}(\mathbf{R}_0)=-I_P$, with I_P the ionization potential of the considered HOMO. In this case, the system of equations (C1) and (C2) has the same complex solutions t_s' and t_s as in the atomic case and obeys the classifications by the indices $s\equiv\{\alpha\beta m\}$ as in [53]. For large internuclear distances, the $\mathbf{R}_0$-dependent terms in the exponents of η_s^q in Eq. (19) should be added to the action, so that $\mathbf{k}_{st}$ and the system (C1) and (C2) contain the $\mathbf{R}_0$-dependent terms. In this case, the saddle-point solutions are characterized by the additional classification numbers, similarly as in [54].

In Fig. 6 we compare the saddle-point and the "exact" harmonic spectra of the N_2 molecule for the same laser parameters as in Fig. 3 and for two values of the angle between the internuclear axis and the laser polarization axis: $\theta_L=0°$ (upper curves) and 45° (lower curves). For the results obtained using the saddle-point method with the first four solutions the harmonic order changes continuously, while for the "exact" results, obtained by numerical integration in Eq. (21), only odd harmonics appear. The agreement is good except for low harmonics and for the harmonic exactly at the cutoff of the corresponding pair of quantum orbits where it is known that the saddle-point method fails which manifests in the form of a spike (this can be avoided using the uniform approximation [53]). The above four-saddle-point approximation, which we use in our numerical calculations in Sec. III, is further justified by the fact that the experimental conditions favor only the solutions with short travel times (the so-called short and long orbits of the Lewenstein model [3]).

APPENDIX D: INTERFERENCE CONDITIONS

Since the T-matrix element given by Eq. (B1) is proportional to $\cos[\mathbf{K}^q(\mathbf{k}_{st},t)\cdot\mathbf{R}_0/2]$ for $s_{a\lambda}=+1$ and $\sin[\mathbf{K}^q(\mathbf{k}_{st},t)\cdot\mathbf{R}_0/2]$ for $s_{a\lambda}=-1$ (see Appendix B), it is straightforward to deduce the following interference conditions:

$$\mathbf{K}^q(\mathbf{k}_{st},t)\cdot\mathbf{R}_0=\begin{cases}(2j+1)\pi & \text{for } s_{a\lambda}=+1,\\ 2j\pi & \text{for } s_{a\lambda}=-1,\end{cases} \tag{D1}$$

where $\mathbf{K}^q(\mathbf{k}_{st},t)$ is given by Eq. (B5) and j is an integer. From Eq. (D1) it follows that the interference condition for the recombination step depends on the dressing of the final state.

If the final molecular bound state is undressed ($q=$u) and $s_{a\lambda}=+1$, using Eq. (B5) we obtain $[k_{st}+A(t)]R_0\cos\theta_L=(2j+1)\pi$, where θ_L is the angle between the internuclear axis and the laser polarization axis. Using Eq. (C2) we finally obtain the following condition for the interference minima for $q=$u and $s_{a\lambda}=+1$:

$$n_{min}^{(u,+1)}=\frac{I_P}{\omega}+\frac{(2j+1)^2\pi^2}{2\omega R_0^2\cos^2\theta_L},\quad j=0,1,\ldots. \tag{D2}$$

Analogously, for $s_{a\lambda}=-1$ we obtain the interference minima condition

$$n_{min}^{(u,-1)}=\frac{I_P}{\omega}+\frac{2j^2\pi^2}{\omega R_0^2\cos^2\theta_L},\quad j=0,1,\ldots. \tag{D3}$$

If the final molecular bound state is dressed ($q=$d) and $s_{a\lambda}=+1$, using Eqs. (B5) and (C2) we obtain $k_{st}R_0\cos\theta_L=(2j+1)\pi$, so that

$$n_{min}^{(d,+1)}=\frac{I_P}{\omega}+\frac{(2j+1)^2\pi^2}{2\omega R_0^2\cos^2\theta_L}+\frac{(2j+1)\pi}{\omega R_0\cos\theta_L}A(t)+\frac{A^2(t)}{2\omega},$$

$$j=0,\pm1,\ldots. \tag{D4}$$

Analogously, for $s_{a\lambda}=-1$ the interference minima condition has the form

$$n_{min}^{(d,-1)}=\frac{I_P}{\omega}+\frac{2j^2\pi^2}{\omega R_0^2\cos^2\theta_L}+\frac{2j\pi}{\omega R_0\cos\theta_L}A(t)+\frac{A^2(t)}{2\omega},$$

$$j=0,\pm1,\ldots. \tag{D5}$$

Therefore, in the case when the final molecular bound state is dressed the interference minima condition contains addi-

tional terms which depend on $A(t)$ and $A^2(t)$, where t is the recombination time. This precludes the observation of clear minima. For some values of t the interference conditions (D4) and (D5) are satisfied so that in the harmonic spectrum we can observe sporadic minima, as can be seen in Figs. 3(a) and 3(c).

Let us now consider the general case of a molecular orbital consisting of atomic orbitals which can have $s_{a\lambda}=+1$ or -1. We will use the notation $a_+ \equiv a(s_{a\lambda}=+1)$ and $a_- \equiv a(s_{a\lambda}=-1)$. According to the results (B1)–(B5) and the saddle-point equations $[\mathbf{k}_{\rm st}+\mathbf{A}(t')]^2=-2I_{\rm P}$ and $[\mathbf{k}_{\rm st}+\mathbf{A}(t)]^2=2(n\omega-I_{\rm P})$ [see Eqs. (C1) and (C2) with $t'=t-\tau$] we obtain that, for a linearly polarized laser field and for the undressed final state, the T-matrix element for emission of the nth harmonic is proportional to

$$I(p,R_0,\theta_{\rm L})\sum_{\alpha\beta m}\tau^{-3/2}e^{i[n\omega t+S_\nu(\mathbf{k}_{\rm st};t,t')]}\hat{\mathbf{e}}_{\rm L}\cdot\hat{\mathbf{e}}^*_{\mathbf{K}} \times\sum_{a'}c_{1a'}\mathbf{m}^*_{a'}(\mathbf{k}_{\rm st},t')\cdot\mathbf{E}(t')F^{q'*}_{s_{a'\lambda}}(\mathbf{k}_{\rm st},t'), \tag{D6}$$

where the multi-index $\alpha\beta m$ denotes the classification of the saddle-point solutions t' and t [53] and

$$p=k_{\rm st}+A(t)=\sqrt{2(n\omega-I_{\rm P})},\quad n\omega>I_{\rm P}. \tag{D7}$$

The interference term $I(p,R_0,\theta_{\rm L})$ is given by

$$I(p,R_0,\theta_{\rm L})=A_+(p,\theta_{\rm L})\cos x-iA_-(p,\theta_{\rm L})\sin x =\sqrt{A_+^2-A_-^2}\,\sin(x+\arctan z), \tag{D8}$$

where

$$2x=pR_0\cos\theta_{\rm L},\quad A_\pm(p,\theta_{\rm L})=\sum_{a_\pm}c_{1a_\pm}\chi'^*_{a_\pm}(p,\theta_{\rm L}),$$

$$z=iA_+/A_-, \tag{D9}$$

and $\chi'_a(p,\theta_{\rm L})\equiv\partial\chi_{n_al_am_a}(\mathbf{p})/\partial p$ is given by Eqs. (A13) and (A14) with $\theta_p=\theta_{\rm L}$, $\phi_p=0$. Therefore, the interference minima condition takes the form $x+\arctan z=j\pi$, so that

$$n^{\rm (u)}_{\rm min}=\frac{I_{\rm P}}{\omega}+\frac{2(j\pi-\arctan z)^2}{\omega R_0^2\cos^2\theta_{\rm L}},\quad j=0,\pm1,\ldots. \tag{D10}$$

For $|z|<1$ we have $\arctan z=z-z^3/3+\cdots$, while for $|z|>1$ it is $\arctan z=\pi/2-1/z+1/(3z^3)-\cdots$. For orbitals having $s_{a\lambda}=+1$ we obtain $1/z=0$ so that $\arctan z=\pi/2$ and Eq. (10) reduces to (D2), while for $s_{a\lambda}=-1$ we have $\arctan z=0$ so that Eq. (D10) reduces to (D3). According to Eqs. (A13) and (A14), for the s and d orbitals having $s_{a\lambda}=+1$ the function $\chi'_a(p,\theta_{\rm L})$ is real, while for the p and f orbitals ($s_{a\lambda}=-1$) it is imaginary. Therefore, the function $z(p,\theta_{\rm L})=iA_+/A_-$ is always real. Since z depends on the harmonic order n through the electron velocity p immediately before the recombination, Eq. (D7), for a fixed angle $\theta_{\rm L}$ Eq. (D10) is a nonlinear equation over n, whose solutions $n^{\rm (u)}_{\rm min}(\theta_{\rm L})$ form a curve in the $(\theta_{\rm L},n)$ plane. These solutions fit well the interference minima obtained numerically [see Figs. 3(b), 3(d), 5(b), and 5(d)].

[1] P. B. Corkum, Phys. Rev. Lett. **71**, 1994 (1993).
[2] K. C. Kulander, K. J. Schafer, and J. L. Krause, in *Super-Intense Laser-Atom Physics*, edited by B. Piraux, A. L'Huillier, and K. Rzążewski, NATO Advanced Studies Institute, Series B: Physics (Plenum, New York, 1993), Vol. 316, p. 95.
[3] M. Lewenstein, Ph. Balcou, M. Yu. Ivanov, A. L'Huillier, and P. B. Corkum, Phys. Rev. A **49**, 2117 (1994).
[4] C. Winterfeldt, C. Spielmann, and G. Gerber, Rev. Mod. Phys. **80**, 117 (2008).
[5] M. B. Gaarde, J. L. Tate, and K. J. Schafer, J. Phys. B **41**, 132001 (2008).
[6] K. Midorikawa, Y. Nabekawa, and A. Suda, Prog. Quantum Electron. **32**, 43 (2008).
[7] T. Pfeifer, M. J. Abel, P. M. Nagel, A. Jullien, Z. H. Loh, M. J. Bell, D. M. Neumark, and S. R. Leone, Chem. Phys. Lett. **463**, 11 (2008).
[8] M. Lein, N. Hay, R. Velotta, J. P. Marangos, and P. L. Knight, Phys. Rev. Lett. **88**, 183903 (2002).
[9] M. Lein, N. Hay, R. Velotta, J. P. Marangos, and P. L. Knight, Phys. Rev. A **66**, 023805 (2002).
[10] R. Kopold, W. Becker, and M. Kleber, Phys. Rev. A **58**, 4022 (1998).
[11] G. Lagmago Kamta and A. D. Bandrauk, Phys. Rev. A **70**, 011404(R) (2004); **71**, 053407 (2005).
[12] T. Kanai, N. Minemoto, and H. Sakai, Nature (London) **435**, 470 (2005).
[13] C. Vozzi, F. Calegari, E. Benedetti, J.-P. Caumes, G. Sansone, S. Stagira, M. Nisoli, R. Torres, E. Heesel, N. Kajumba, J. P. Marangos, C. Altucci, and R. Velotta, Phys. Rev. Lett. **95**, 153902 (2005).
[14] J. Itatani, J. Levesque, D. Zeidler, H. Niikura, H. Pépin, J. C. Kieffer, P. B. Corkum, and D. M. Villeneuve, Nature (London) **432**, 867 (2004).
[15] M. Lein, J. Phys. B **40**, R135 (2007).
[16] J. Levesque and P. B. Corkum, Can. J. Phys. **84**, 1 (2006).
[17] A. Scrinzi, M. Yu. Ivanov, R. Kienberger, and D. M. Villeneuve, J. Phys. B **39**, R1 (2006).
[18] G. N. Gibson and J. Biegert, Phys. Rev. A **78**, 033423 (2008).
[19] M. Lein, P. P. Corso, J. P. Marangos, and P. L. Knight, Phys. Rev. A **67**, 023819 (2003).
[20] D. A. Telnov and Shih-I Chu, Phys. Rev. A **76**, 043412 (2007).
[21] I. A. Gonoskov and M. Yu. Ryabikin, J. Mod. Opt. **55**, 2685 (2008).
[22] M. F. Ciappina, C. C. Chirilă, and M. Lein, Phys. Rev. A **75**, 043405 (2007).
[23] B. Zimmermann, M. Lein, and J. M. Rost, Phys. Rev. A **71**, 033401 (2005).
[24] Y. Mairesse, J. Levesque, N. Dudovich, P. B. Corkum, and D.

M. Villeneuve, J. Mod. Opt. **55**, 2591 (2008).
[25] D. B. Milošević, Phys. Rev. A **74**, 063404 (2006).
[26] M. Busuladžić, A. Gazibegović-Busuladžić, D. B. Milošević, and W. Becker, Phys. Rev. Lett. **100**, 203003 (2008); Phys. Rev. A **78**, 033412 (2008).
[27] W. Becker, J. Chen, S. G. Chen, and D. B. Milošević, Phys. Rev. A **76**, 033403 (2007).
[28] C. B. Madsen and L. B. Madsen, Phys. Rev. A **74**, 023403 (2006).
[29] V. I. Usachenko, P. E. Pyak, and Shih-I Chu, Laser Phys. **16**, 1326 (2006).
[30] J. Chen and S. G. Chen, Phys. Rev. A **75**, 041402(R) (2007).
[31] O. Smirnova, M. Spanner, and M. Ivanov, J. Mod. Opt. **54**, 1019 (2007).
[32] C. C. Chirilă and M. Lein, Phys. Rev. A **73**, 023410 (2006); **77**, 043403 (2008).
[33] C. Figueira de Morisson Faria, Phys. Rev. A **76**, 043407 (2007).
[34] A.-T. Le, R. Della Picca, P. D. Fainstein, D. A. Telnov, M. Lein, and C. D. Lin, J. Phys. B **41**, 081002 (2008); T. Morishita, A.-T. Le, Z. Chen, and C. D. Lin, Phys. Rev. Lett. **100**, 013903 (2008); V.-H. Le, N.-T. Nguyen, C. Jin, A.-T. Le, and C. D. Lin, J. Phys. B **41**, 085603 (2008).
[35] R. Santra and A. Gordon, Phys. Rev. Lett. **96**, 073906 (2006); A. Gordon, F. X. Kärtner, N. Rohringer, and R. Santra, *ibid.* **96**, 223902 (2006).
[36] S. Patchkovskii, Z. Zhao, T. Brabec, and D. M. Villeneuve, Phys. Rev. Lett. **97**, 123003 (2006); J. Chem. Phys. **126**, 114306 (2007).
[37] D. Bauer, D. B. Milošević, and W. Becker, Phys. Rev. A **72**, 023415 (2005).
[38] D. B. Milošević, in *Super-Intense Laser-Atom Physics*, edited by B. Piraux and K. Rzążewski, (Kluwer, Netherlands, 2001), p. 229.
[39] D. B. Milošević and F. Ehlotzky, Adv. At., Mol., Opt. Phys. **49**, 373 (2003).
[40] V. N. Ostrovsky, J. Phys. B **38**, 4399 (2005).
[41] O. Smirnova, S. Patchkovskii, and M. Ivanov (unpublished).
[42] If the internuclear distance changes on the time scale of the electron travel time, then the dynamic two-center interference is possible. It has been recently observed in HHG from the H_2 molecule that the interference occurs at lower harmonic order than would be the case if the nuclei were static: S. Baker, J. S. Robinson, M. Lein, C. C. Chirilă, R. Torres, H. C. Bandulet, D. Comtois, J. C. Kieffer, D. M. Villeneuve, J. W. G. Tisch, and J. P. Marangos, Phys. Rev. Lett. **101**, 053901 (2008).
[43] S. Ramakrishna and T. Seideman, Phys. Rev. Lett. **99**, 113901 (2007); Phys. Rev. A **77**, 053411 (2008); F. H. M. Faisal and A. Abdurrouf, Phys. Rev. Lett. **100**, 123005 (2008).
[44] For the atomic systems it is known that the application of the saddle-point method to the integral over the intermediate electron momenta is a good approximation [see, for example, D. B. Milošević and B. Piraux, Phys. Rev. A **54**, 1522 (1996)]. For molecular systems this has been recently checked by performing explicit integration over $d^3\mathbf{k}$ [C. C. Chirilă and M. Lein, (unpublished)]. Only the minima in HHG spectra and the phase jumps of the corresponding harmonic phase for particular molecular orientation become less sharp in comparison with the results obtained using the saddle-point method.
[45] A.-T. Le, X.-M. Tong, and C. D. Lin, Phys. Rev. A **73**, 041402(R) (2006); J. Mod. Opt. **54**, 967 (2007); P. Liu, P. Yu, Z. Zeng, H. Xiong, X. Ge, R. Li, and Z. Xu, Phys. Rev. A **78**, 015802 (2008).
[46] It should be mentioned that in our calculations we use the saddle-point method so that the harmonic order changes continuously and we obtain $n_{\min}=44.1$ and $n_c=70.1$. Calculations are fast and the whole spectrum is obtained in a few seconds on a standard personal computer. In [8,9] a trapezoidally shaped laser pulse with a total duration of ten optical cycles and linear ramps of three optical cycles was used and calculations were time consuming.
[47] This wavelength corresponds to the effective plane wave having the energy $E_k=k^2/2=n_{\min}\omega$, $\lambda=2\pi/k$ [9,15]. The use of this "dispersion relation," instead of the usual dispersion relation $E_k+I_P=n_{\min}\omega$ that emerges from the simple man's model (this is the energy-conserving condition at recombination time), is heuristically justified in Refs. [9,15] by the influence of the attractive long-range binding potential in the core region. However, we obtain the correct results without such a correction. As explained in the text, the interference of even and odd atomic orbital contributions during the recombination of the returned electron's wave packet leads to the correct position of the interference minima.
[48] A. C. Wahl, P. E. Cade, and C. C. J. Roothaan, J. Chem. Phys. **41**, 2578 (1964).
[49] A. C. Wahl, J. Chem. Phys. **41**, 2600 (1964).
[50] P. E. Cade, K. D. Sales, and A. C. Wahl, J. Chem. Phys. **44**, 1973 (1966).
[51] P. E. Cade and A. C. Wahl, At. Data Nucl. Data Tables **13**, 339 (1974).
[52] A. C. Wahl and R. H. Land, J. Chem. Phys. **50**, 4725 (1969).
[53] D. B. Milošević and W. Becker, Phys. Rev. A **66**, 063417 (2002).
[54] S. Odžak and D. B. Milošević, Phys. Rev. A **72**, 033407 (2005).